

Modeling and Analysis of Meteorological Contour Matching with Remote Sensor Data for Navigation

Louis A. Catalano ¹, Zhiyong Hu ², Hakki Erhan Sevil ^{3,*}

¹ Catalano Aerospace, Pensacola, FL 32514, USA; catalanoaerospace@gmail.com

² Earth and Environmental Sciences, University of West Florida, Pensacola, FL 32514, USA; zhu@uwf.edu

³ Intelligent Systems & Robotics, University of West Florida, Pensacola, FL 32514, USA

* Correspondence: hsevil@uwf.edu

Abstract: This paper outlines the methods, results, and statistical analysis of a model we developed to demonstrate the feasibility of applying remote sensor meteorological data to navigation by using meteorological contour matching (METCOM). Terrain contour matching (TERCOM), a contemporary navigation system, possesses inherent performance flaws that may be resolved and improved by METCOM for subsonic and hypersonic missile or aircraft navigation. Remote sensor imagery data for this model was accessed from the Geostationary Operational Environmental Satellites-R Series operated by the National Oceanic and Atmospheric Administration by using Amazon Web Services through a script we developed in Python. Data processed for the model included imagery data and corresponding geospatial data from the legacy atmospheric profile products: legacy vertical temperature and legacy vertical moisture. Our analysis of the model included an error assessment to determine model accuracy, geostatistical analysis through semivariograms, meteorological signal of model data, and a combinatorial analysis to evaluate navigation performance. We conducted a model assessment which indicated an accuracy of 66.2% in the data used as a combined result of instrument error and interference of cloud formations. Results of the remaining analysis offered methods to evaluate METCOM performance and compare different meteorological data products. These results allowed us to statistically compare METCOM and TERCOM, yielding several indications of improved performance including an increase by a factor of at least 13.5 in data variability and contourability. The analysis we conducted served as a proof of concept to justify further research into the feasibility and application of METCOM.

Keywords: remote sensing; meteorology; climate; geo-statistics; data science; navigation systems



Citation: Catalano, L.A.; Hu, Z.; Sevil, H.E. Modeling and Analysis of Meteorological Contour Matching with Remote Sensor Data for Navigation. *Automation* **2022**, *3*, 302–314. <https://doi.org/10.3390/automation3020016>

Received: 21 April 2022

Accepted: 8 June 2022

Published: 13 June 2022

Publisher's Note: MDPI stays neutral with regard to jurisdictional claims in published maps and institutional affiliations.



Copyright: © 2022 by the authors. Licensee MDPI, Basel, Switzerland. This article is an open access article distributed under the terms and conditions of the Creative Commons Attribution (CC BY) license (<https://creativecommons.org/licenses/by/4.0/>).

1. Introduction

Reliable, cost-effective precision navigation is a key research concentration for many defense organizations. The recent emergence of hypersonic weapons development further reinforces the demand for accurate and affordable navigation systems [1]. A current and widely implemented method of navigation is terrain contour matching (TERCOM) [2,3]. Despite its name, modern TERCOM actually matches altitude by comparing the current altitude of the missile with the elevation of the terrain by utilizing a combination of radar, baro-altimeter, and temperature sensors. Data collected from these instruments are correlated with preloaded terrain elevation data typically sourced from topographic charts or aerial photography. This data is stored in a numeric matrix of discrete “cells” that represent terrain elevation. Data correlation allows the missile to correct any drift incurred during flight and navigate the missile back to its intended track [2].

TERCOM, however, has notable system errors and operational setbacks. For example, TERCOM loses accuracy at higher altitudes as radar becomes less effective for terrain correlation [2]. As a consequence, TERCOM is impractical for high-altitude flight, typical of hypersonic weapon systems. TERCOM is also vulnerable to data errors caused by

obstructions over terrain including snow, trees, buildings, and foliage [2,3]. Additionally, the effectiveness of TERCOM is largely dependent on terrain roughness which renders it unreliable over flat or smooth areas such as bodies of water. Therefore, TERCOM is often combined with other navigation systems such as the Inertial Navigation System (INS) and the Global Positioning System (GPS) [2]. Yet, introducing additional navigation systems to a weapon platform naturally increases the cost to operate and maintain [2,3]. The goal of this model is to prove the feasibility of a navigation system that expands on the shortcomings of TERCOM and as a result, provides a cost-effective yet more reliable alternative for subsonic and hypersonic navigation systems.

Recent developments in remote sensing have significantly increased the accuracy and reliability of collected meteorological data. Current satellite and aircraft remote sensing systems can provide near-real-time images with spatial resolutions as small as 0.5 to 2.5 m [4]. Further advancements in microwave and infrared radiometry have allowed sensors to measure the vertical profile of atmospheric temperatures, humidity, and ozone concentrations. Future development and deployment of hyperspectral imaging will further enhance spatial resolution and accuracy of remote sensing [5]. Similar to TERCOM, remote sensor images are typically processed by using a raster model that is stored and manipulated in a three-dimensional numeric matrix. The dimensions usually consist of two or three spatial coordinates and a spectral dimension [5]. Similar to terrain contouring, meteorological data can also be contoured through isobars and isotherms to display horizontal and vertical profiles of pressure and temperature, respectively.

The theory explored in this paper is that remote sensor meteorological data can be contoured and matched in real-time by using meteorological sensors onboard a missile or aircraft; this process is illustrated in Figure 1. The data collected by the remote sensor in step 1 would be transmitted to the missile or aircraft either directly or through a control station as shown in step 2. The meteorological data measured by instrumentation onboard the missile or aircraft in step 3 would then be matched with the transmitted satellite data in step 4. Like TERCOM, the navigation system would match the datasets to correct for drift and ultimately navigate the missile or aircraft to its intended destination. The contour matching could be applied to missile or aircraft navigation and improve on the setbacks of TERCOM. We verified the feasibility of this concept through a sample model statistical comparison with TERCOM. The model developed applied atmospheric temperature and moisture to serve as a proof of concept for methods to evaluate and simulate a navigation system based solely on meteorological contour matching (METCOM).

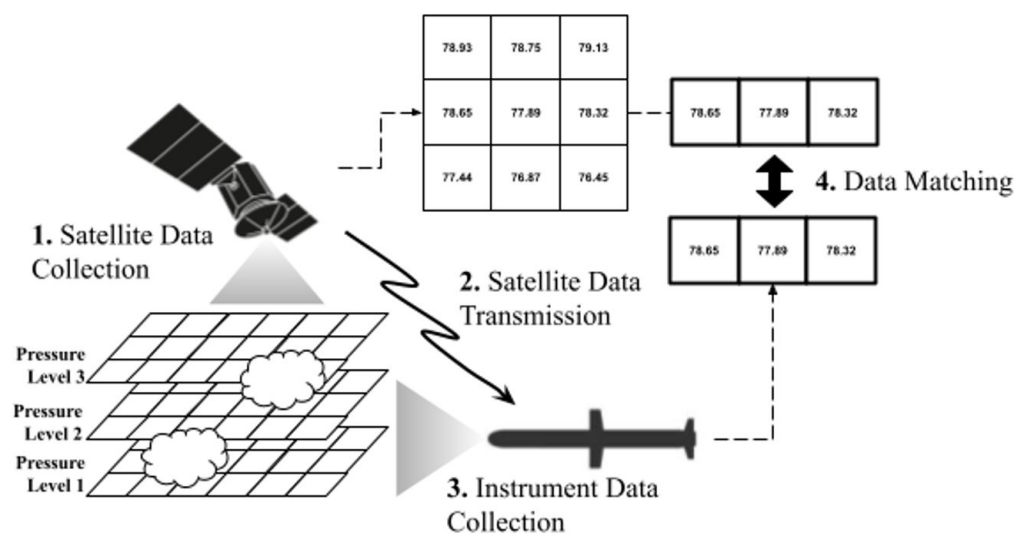


Figure 1. Meteorological Contour Matching (METCOM) data process.

2. Details of Datasets

2.1. Remote Sensor Data

The data sensor that we chose for this model was the Geostationary Operational Environmental Satellites-R (GOES-R) Series operated by the National Oceanic and Atmospheric Administration (NOAA) to collect meteorologic imagery of the United States. The GOES-R's primary sensor is an Advanced Baseline Imager (ABI) in addition to several other secondary sensors. The ABI is a 16 spectral band radiometer that images Earth's weather, oceans, and environments [4]. Currently within the GOES-R Series there are two operational satellites. We selected the GOES-16 Level 2+ Mode 6 satellite which can provide full disk imagery (FDI) of the earth at a spatial resolution of 0.5 to 10 km [5].

2.2. Spatial Data

Spatial data of the imagery we used for this model is from GOES-EAST which covers the eastern portion of the Western hemisphere. For reference, Figure 2 displays the spatial area of the FDI corresponding with the model; this image was sourced directly from GOES-R's website [6].



Figure 2. Model spatial area [6].

ABI Level 2+ products are on an ABI fixed grid projected to a GRS80 ellipsoid which allows for data points from every product to be located at the same point on earth [5]. The ABI fixed grid is defined by the angular separation between each data point originating from the satellite; this angle is also the basis for horizontal spatial resolution. The horizontal spatial resolution of the products selected for this model is 10 km, which is 280 microradians of angular separation [4].

Vertical resolution is also relevant for the products that we handled in this model: legacy vertical moisture and legacy vertical temperature. Both products have a vertical dimension with a resolution of 3 to 5 km. Vertical data points are measured on 101 standard pressure levels which are listed in Figure 3, thus totaling 119,118,996 data points for each product [4].

Level	Pressure (hPa)	Level	Pressure (hPa)	Level	Pressure (hPa)	Level	Pressure (hPa)
1	1100.0	26	496.6298	51	151.2664	76	18.5847
2	1071.917	27	477.9607	52	142.3848	77	16.4318
3	1042.232	28	459.7118	53	133.8462	78	14.4559
4	1013.948	29	441.8819	54	125.6456	79	12.6492
5	986.0666	30	424.4698	55	117.7775	80	11.0038
6	958.5911	31	407.4738	56	110.2366	81	9.5119
7	931.5236	32	390.8926	57	103.0172	82	8.1655
8	904.8659	33	374.7241	58	96.1138	83	6.9567
9	878.6201	34	358.9665	59	89.5204	84	5.8776
10	852.788	35	343.6176	60	83.231	85	4.9204
11	827.3713	36	328.6753	61	77.2396	86	4.077
12	802.3714	37	314.1369	62	71.5398	87	3.3398
13	777.7897	38	300.0	63	66.1253	88	2.7009
14	753.6275	39	286.2617	64	60.9895	89	2.1526
15	729.8857	40	272.9191	65	56.126	90	1.6872
16	706.5654	41	259.9691	66	51.5278	91	1.2972
17	683.6673	42	247.4085	67	47.1882	92	0.9753
18	661.192	43	235.2338	68	43.1001	93	0.714
19	639.1398	44	223.4415	69	39.2566	94	0.5064
20	617.5112	45	212.0277	70	35.6505	95	0.3454
21	596.3062	46	200.9887	71	32.2744	96	0.2244
22	575.5248	47	190.3203	72	29.121	97	0.137
23	555.1669	48	180.0183	73	26.1829	98	0.0769
24	535.2322	49	170.0784	74	23.4526	99	0.0384
25	515.72	50	160.4959	75	20.9224	100	0.0161
						101	0.005

Figure 3. Vertical data pressure levels [4].

2.3. Imagery Data

The GOES-16 provides imaging data for each of the 16 spectral bands including visible, near-infrared, and infrared imagery [4]. We collected two products for the model: legacy vertical moisture (LVM) and legacy vertical temperature (LVT) which are both part of the legacy atmospheric profile (LAP). Table 1 displays more product information provided by GOES-R. LAP products produce data under “clear sky” conditions which is defined by GOES-R’s Cloud Mask algorithm. The algorithm is an intermediate level-4 cloud mask that identifies pixels on a spectrum from “clear” to “cloudy” [7]. Both LAP products contained horizontal and vertical imagery data necessary for the model.

Table 1. Model imaging Cartesian coordinate bounds [4].

Product Name	Data Range	Data Dimensions (y, x, Pressure Level)	Measurement Accuracy at Altitude Ranges	Measurement Precision at Altitude Ranges
Legacy Vertical Moisture	0–100%	1086, 1086, 101	Surface to 500 hPa: 18%	Surface to 500 hPa: 18%
			500 to 300 hPa: 18%	500 to 300 hPa: 18%
Legacy Vertical Temperature	180–320 K	1086, 1086, 101	300 hPa to 100 hPa: 20% 1 K below 400 hPa and above boundary layer	300 hPa to 100 hPa: 20% 2 K below 400 hPa and above boundary layer

3. Meteorological Contour Matching Pipeline

3.1. Data Access

There are numerous methods by which to access and process data from GOES-R [8]. Python 3.10, an object-oriented programming language, is widely used for handling data from GOES-R and offered the necessary functions for this analysis. Real-time data from GOES-R can be accessed from several different repositories, but for this model, Amazon Web Services (AWS) provided a channel to the desired datasets in the form of NetCDF4 files [8]. NetCDF4 or Network Common Data Form is an array-oriented data format commonly utilized to store large amounts of geospatial information [4]. The Python script we wrote for this model first called the requested datasets from AWS using anonymous credentials. Then, we downloaded the files locally where the data was made available for index within the Python script.

3.2. Data Validation

All data provided by GOES-R is validated under a specific set of requirements by their algorithm integration team [7]. However, in this study, we conducted additional error analysis for navigation performance evaluation. GOES-R identifies several sources of data error including inaccuracies in the Cloud Mask algorithm, instrument noise, background, radiance and calibration bias. By using a covariance analysis, GOES-R provides the measurement accuracy of each product as shown in Table 1 [4]. In addition to measurement error, there are masked spectral elements within the matrices that would degrade navigation accuracy. These empty cells are data points identified by the Cloud Mask algorithm as “cloudy” and therefore the data is not available. Remote observations are typically impeded by oxygen, ozone, water vapor, and carbon dioxide in the atmosphere that absorb and scatter sensor radiation [5,7,9]. Hence, the contributions of these effects were taken into account for the analysis.

We plotted model imagery data for both products in Figure 4 for a visual illustration at pressure level 1. The figure also visually signifies the amount of null data at this level represented by the colorless area of the disk. The nullity at every level for each dataset was measured by using a simple filter in the Python script. We also conducted a temporal analysis of the data in order to account for any variables that may affect cloud coverage over time such as wind direction and sunlight. Data was studied on hourly and monthly intervals. AWS only archives imagery data within two years of the current date, so an annual analysis was not possible; however, based on the results from the hourly and monthly data, a yearly analysis was deemed unnecessary. For the model and remainder of the analysis, the data we used was from 2 July 2021 at 00:00 Greenwich Mean Time (GMT) which reflected a percent nullity similar to the monthly average.

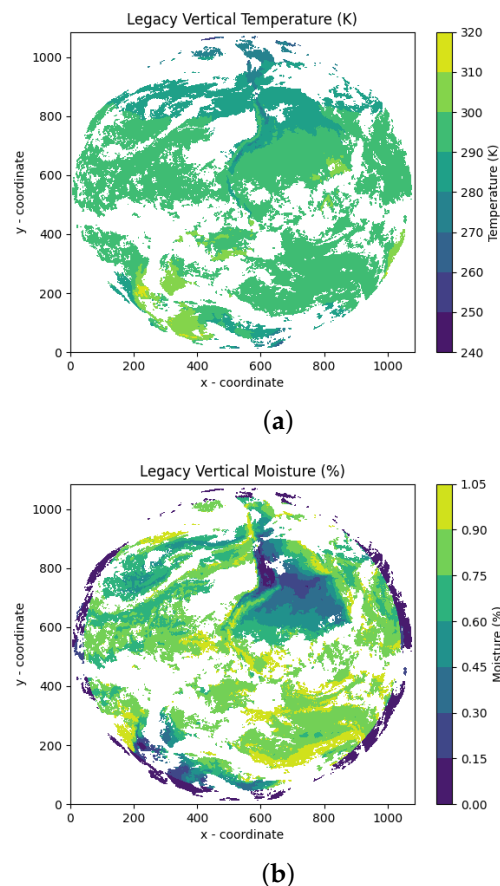


Figure 4. Pressure level 1 plots of model imagery data on 2 July 2021 at 00:00:00 GMT. (a) Temperature (K) (b) Moisture (%).

3.3. Data Process

Data validation permitted further processing for the navigation performance analysis. One method to offset the effect of null data on METCOM performance is by incorporating additional datasets. Unlike TERCOM, which only measures terrain elevation, METCOM can corroborate data from more than one source, and in the case of this model the data are temperature and moisture. To evaluate the performance of METCOM under numerous datasets, we conducted a combinatorial analysis of the model. The percent of missing data or percent nullity was used to model the probability that a geospatial coordinate contains a masked cell. Therefore, we measured the performance of METCOM under multiple datasets by using the multiplicative probability of nullity. To illustrate this relationship, the percent of missing data was plotted against an increasing number of datasets in figure in Section 4.2.

Subsequent methods to assess METCOM performance subsist through a geostatistical analysis. Geostatistics is a specialized form of statistics that studies variables spatially and temporally and is commonly used for mining and occasionally for weather prediction [10]. We used a geostatistical model called the semivariogram to study the horizontal meteorological data, that is, the data which was observed within the same pressure level. The semivariogram graphically and empirically estimates the relation between the value of a variable and its spatial reference to other variables. The analysis is simple but fundamental in determining the ability to contour meteorological data. For this model, the amount of data collected was substantial and, in its entirety, unnecessary for the variogram analysis. Therefore, the semivariograms we generated for this analysis were sample semivariograms encompassing only a portion of the horizontal model population data shown in the first figure in Section 4.3. The sample sizes were determined by using an acceptable confidence level and margin of error.

The vertical meteorological data, the data distributed across several pressure levels, was not analyzed through a variogram analysis. Meteorological conditions such as temperature and moisture already have a well-studied relationship with altitude; thus, a variogram would not offer any compelling information to this analysis. Instead, we plotted temperature and moisture with pressure in the second figure in Section 4.3 to observe the vertical profile of the meteorological conditions and estimate data variability as an indicator of contourability.

METCOM performance was measured with the same method used for assessing the performance of TERCOM where the standard deviation of terrain elevation represents terrain roughness. This method has been historically applied to TERCOM performance for both simulated and real terrain [2,9]. The standard deviation of the meteorological data is also called the meteorological signal. Meteorological signals can be viewed as the discrete entropic behavior of weather and climate. Thus, for METCOM, we applied the standard deviation of meteorological data to quantify meteorological signals as an indication of performance. In order to draw a comparison between the signals of METCOM and TERCOM, we determined their respective coefficients of variation. The coefficient of variation simply normalizes the standard deviation by the mean, which allows for variability to be compared between datasets of scaled values with different means [11]. The coefficient of variation is similar to the signal-to-noise ratio of image processing, which is another metric used to assess TERCOM performance [12].

4. Performance Analysis and Results

4.1. Accuracy & Precision

The first set of results from the model was the accuracy and precision that we derived from the data validation. The percent accuracy of both products in the model was calculated from the provided measurement accuracy and the percent of “cloudy” or missing data. The percent of nullity for the products in the model was 66.234% or 40,222,038 data points. It is clear that the majority of the model data contained missing data which accounted for approximately 7,811,580 cubic kilometers of Earth’s atmosphere. Yet, this deceptively large volume is only about 0.372% of Earth’s hemispherical atmosphere. Figure 5 displays the monthly percent of missing data during 2021; the mean was 65.408% with a standard

deviation of 2.182%. Over a year's time span, the percent nullity did not vary significantly so it can be concluded that seasonal changes do not greatly influence the data. Figure 6 shows the percent of missing data over the course of a single day with a mean of 67.007% and a standard deviation of 1.731%. Once again, the percent nullity is relatively constant, providing the supposition that sunlight also does not affect the data. A yearly analysis was not feasible due to constraints from the AWS data repository; thus an investigation may be warranted in future research, especially a study on the potential impact that climate change may have on METCOM performance.

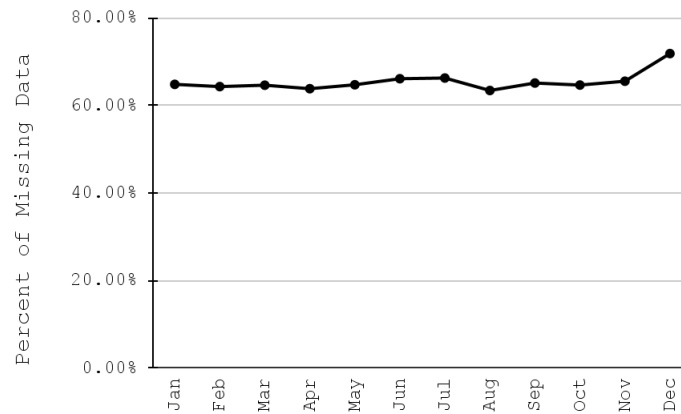


Figure 5. Monthly percent of missing data in 2021.

The percent accuracy and precision resulting from the missing data is presented in Table 2 in addition to the measurement accuracy and precision provided by GOES-R [4]. LVM is notably less accurate and precise than LVT. Thus, the selection of other types of meteorological or climate data may provide greater performance. The presence of missing data is the largest contributor to model inaccuracy; therefore, any practical applications of METCOM would benefit from a more refined cloud mask algorithm and/or utilizing a sensor capable of penetrating cloud canopies that conceal meteorological data.

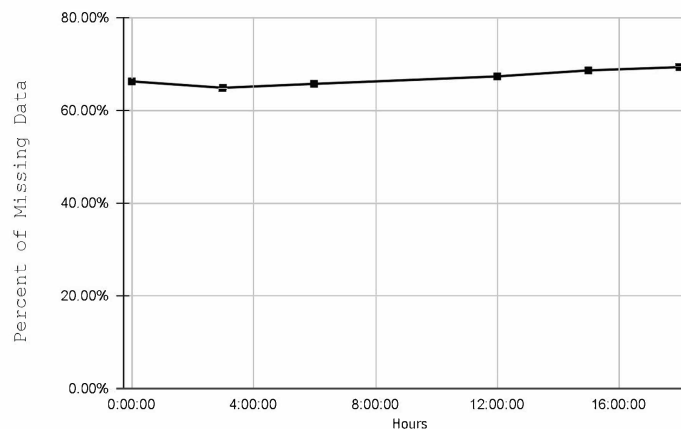


Figure 6. Hourly percent of missing data on 2 July 2021.

Table 2. Percent accuracy and precision of model data.

	Percent Accuracy	Percent Precision
LVT Measurement	99.286%	98.571%
LVM Measurement	80.000%	80.000%
Null Data	66.234%	74.100%

4.2. Combinatorial Analysis

The combinatorial analysis yielded an anticipated exponential relationship between the number of datasets and the percent of missing data shown in Figure 7. This analysis assumed that each additional dataset possessed the same percent nullity and standard deviation of the LAP products used in the model. Therefore, it is expected that supplemental datasets with lower percentages of null data will obviously converge with fewer datasets.

The purpose of the combinatorial analysis is to model the expected behavior and method for determining METCOM performance with increasing sets. These may include alternative meteorological or climate data collect from remote sensors such as ozone, wind motion, aerosol, cloud particle size, dust, air mass reflectance, separation, and carbon dioxide.

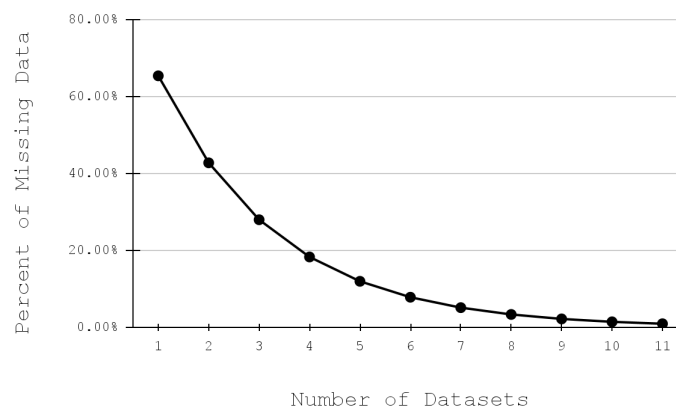


Figure 7. Multiplicative percent nullity versus number of datasets.

This list is just a portion of potential data sources that can contribute to the horizontal and vertical profiles of METCOM [4]. In addition, for weapon systems that demand a more discrete surface solution, the following surface datasets can be incorporated: vegetation density, soil reflectance, surface color, surface temperature, subterranean magnetic anomaly, and surface winds.

Additionally, many remote sensors, GOES-R included, have oceanography products that take measurements including wave height, wave frequency, sea surface temperature, sea ice thickness, sea ice concentration, ocean color, sea salinity, and chlorophyll [4].

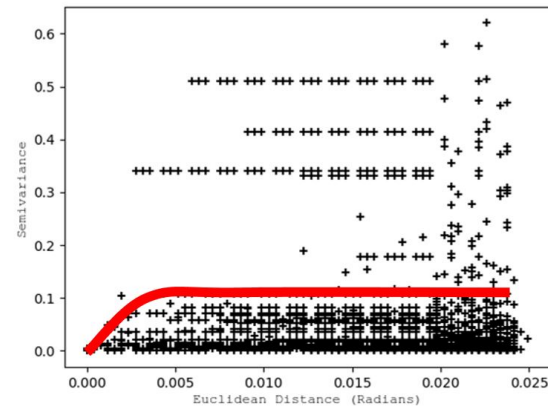
Each of these products could provide data for a sea surface solution especially crucial for weapons-guidance systems that engage in sea surface warfare. Nevertheless, the actual viability of each product for use in navigation is unknown but proves that there at least exist remote sensor products that can potentially improve the performance of METCOM and may be validated in future research.

4.3. Geostatistical Analysis

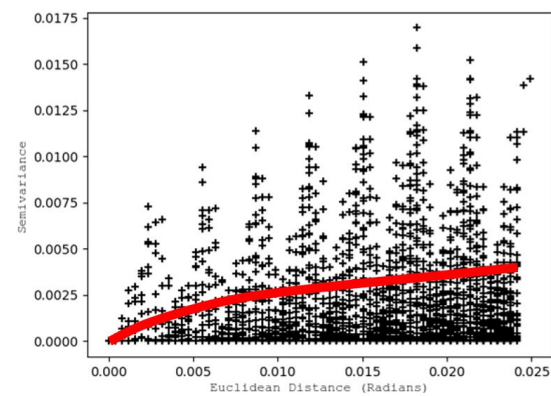
To assess the horizontal spatial dependence of the meteorological data used in the model, sample semivariograms of each product were depicted in Figure 8 by using a script we wrote in Python. The horizontal semivariograms were based on samples of the model data at the first pressure level. The sample size for both products was 68 data points with a 90% confidence level and a 10% margin of error. Accordingly, the samples for both semivariograms independently covered a randomly selected area of approximately 680 square kilometers. The sample mean and sample variance can be found in Table 3.

Table 3. Model horizontal sample semivariogram data.

Sample Semivariogram	Sample Size	Sample Mean	Sample Variance	Model Behavior	Sill	Range
Horizontal LVT	68	297.809 K	0.181 K	Spherical	0.100	0.005 rad
Horizontal LVM	68	57.653%	3.461%	Exponential	0.003	0.00285 rad



(a)



(b)

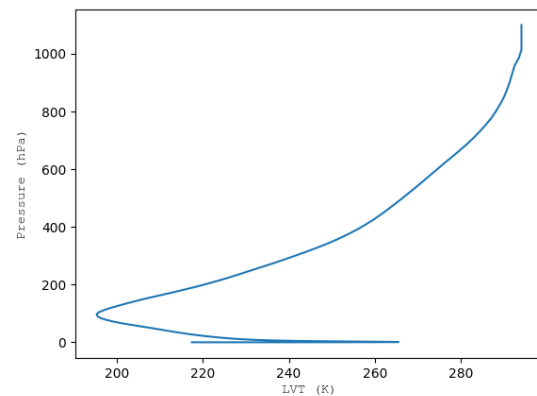
Figure 8. Horizontal sample semivariogram of LVT (a) and LVM (b) at pressure level 1.

The horizontal sample semivariograms we generated in Python plotted the Euclidean distance against the squared difference or semivariance of the data in Figure 8. The Euclidean distance is the geospatial distance between each and every data point within the sample. The semivariograms display the nugget, simply the data point at (0,0), which indicates an expected zero lag. The solid red line portrays an estimated model to approximate the data's spatial relationship. Table 3 also lists the model behavior of each variogram. The spherical model behavior of LVT was expected because this model is typical for geopotential differential variables in meteorology [10]. LVM displayed an exponential behavior indicating that the variability had no “recall force” as it infinitely increased with distance. The sill of a variogram is the value at which the graph levels off. The distance where the sill begins is called the range, signifying that the data is no longer spatially correlated; the range was used as a measure of the capacity for a dataset to be contoured [10]. Both the sill and range of the semivariograms are provided in Table 3.

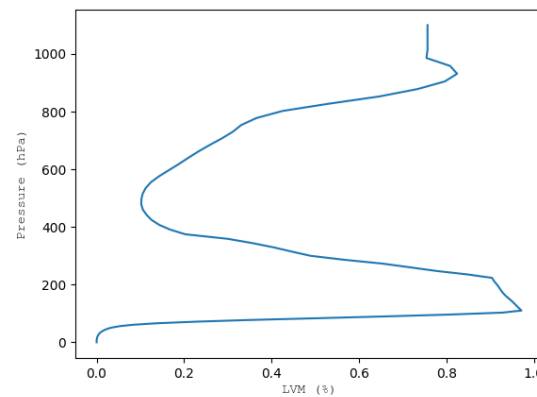
The horizontal semivariograms had indicated that LVM is a better dataset than LVT for contouring in accordance to their ranges. The range of the spherical model is visually simple to determine; for exponential models, however, an accepted method for finding the range is to use 95% of the sill [10]. The horizontal range of LVT converted roughly to 178.571 km

and the horizontal range of LVM was 101.786 km. Therefore, if the meteorological data were to be plotted on a contour map, the separation between each isotherm and isohume would be the ranges of LVT and LVM, respectively.

The vertical meteorological data was plotted in Figure 9 for both products. Note that the y-axis is plotted as increasing pressure, which is a decrease in altitude. LVT and LVM displayed distinct yet expected relationships with altitude. The variability of vertical data can be assessed by observing the slope of the profile. A greater slope indicates a greater change in value with altitude; LVT is clearly more discreet than LVM in this regard. Additionally, LVM has repeating values with altitude. Thus, in terms of vertical variability, LVT is a better candidate than LVM, which is contrasting to the horizontal contourability analysis. Nevertheless, in practice, horizontal variability is of greater importance than vertical variability because longitudinal and latitudinal coordinates change at greater rates than altitude during missile flight [2]. This is also additional evidence that METCOM can offer greater performance when combining several products.



(a)



(b)

Figure 9. Vertical data distribution of LVT (a) and LVM (b) over atmospheric pressure.

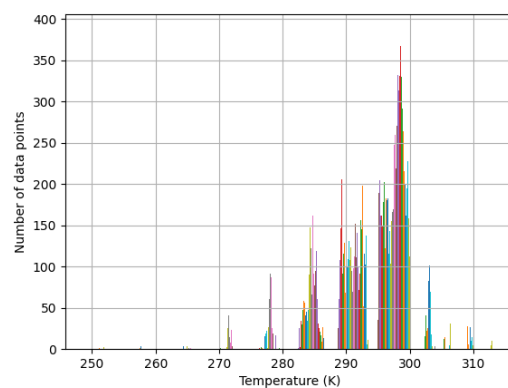
4.4. METCOM versus TERCOM

To compare the performance of METCOM and TERCOM, the coefficient of variation allowed for the meteorological signals of different means to be compared with the terrain roughness of TERCOM. The meteorological signals, analogous with the standard deviations, were found for both products [11]. The standard deviation and population mean of the LVT data was 29.555 K and 243.054 K respectively. For LVM, the standard deviation was 28.011% and 23.163% was the calculated population mean. The resulting coefficient of variation for the LVM was 0.122 and 1.209 for LVM. The coefficient of variation for TERCOM was determined by using a standard deviation of 25 feet which is the minimum standard deviation required by design for TERCOM [2]. The mean value used was the world terrain

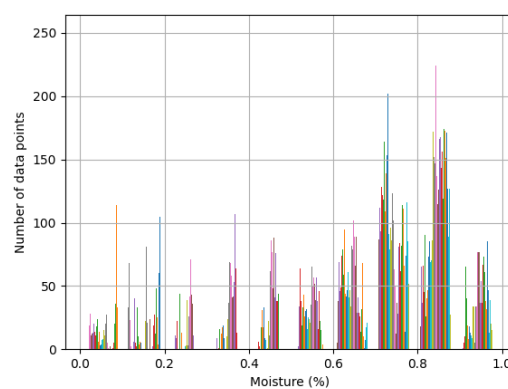
elevation average of 2756 feet [13]. Therefore, the corresponding coefficient of variation was 0.009 for TERCOM. Clearly, the variability of each individual meteorological dataset was substantially greater than that of terrain elevation, by a factor of approximately 13.5 for LVT and 134 for LVM. The meteorological signals we found were indicators of improved performance and may be an indicator for other products as well, such as those listed in Section 4.2, to assess navigation performance.

Figure 10 is a histogram plot of the data distribution for both model products at the first pressure level. These graphs provided an example of two contrasting distributions. Temperature had a negatively skewed tendency whereas moisture's distribution was slightly negatively skewed but more dispersed with outliers. This was verified empirically by the coefficients of variation calculated. Consequently, it was statistically and graphically proven that moisture was a better data candidate for METCOM than temperature when exclusively considering variability. Larger variability in meteorological data indicates areas of potentially more fixes for contour matching. If the data lacks variability, then it would be increasingly difficult for a navigation system to distinguish location [2].

As with any statistical analysis, this comparison was based on some assumptions that must be discussed regarding this comparison. The meteorological dataset only incorporated the Western hemisphere while the terrain data was measured over the entire globe. However, it can be reasonably assumed that even on a global scale, meteorological variability is still greater than terrain variability. A rational explanation for such a drastic difference in variation is likely related to the fact that two-thirds of the world's surface is covered by water where elevation variability is virtually constant [13].



(a)



(b)

Figure 10. Model data distribution of LVT (a) and LVM (b) at the surface.

There are, however, several factors that must be considered in order for METCOM to be competitive against TERCOM. One drawback of greater data variability and multiple

data sources is its greater demand on computer memory and processing. Memory limitations are one of the setbacks that restrict the accuracy of TERCOM [3]. Therefore, future development of METCOM will need to focus on effective data management in order to minimize cost while maximizing accuracy. An additional concern for any remote sensor navigation system is the increasing threat to satellites in modern cyberwarfare [1]. However, recent developments in weather and climate simulation can generate meteorological prediction models with great accuracy independent of satellite technology [9]. Navigation based entirely on simulated or modeled data is inherently risky, especially for missiles, but METCOM may offer a reliable platform for its application. Moreover, the expanding capabilities of artificial intelligence and machine learning can significantly advance meteorological modeling and simulation for METCOM performance. Regardless, the results of this research have marked a promising introduction to a novel method of navigation.

5. Conclusions

A recent surge in hypersonic weapons development demands a new suite of navigation systems that can keep pace. METCOM offers a unique approach to geospatial navigation with noticeable potential for performance. Resulting analysis shows that, statistically, METCOM can improve on the performance of terrain contour-matching navigation by a significant factor. The model proved that METCOM could provide discrete locations by matching meteorological data gathered by remote sensors independent of terrain variability. However, this model is a proof of concept and beckons for additional research to further confirm viability of navigation for not only missiles but potentially aircraft, spacecraft, and all air vehicles. Advancements in remote sensing technology and increased integration of artificial intelligence in weapon systems may further validate METCOM as a reliable method of navigation. Future research should include a systems analysis of METCOM with current missile and aircraft avionics and control systems. A study into incorporating different remote sensor platforms and weather/climate data as well as simulation methods may further legitimize the performance and cost effectiveness of METCOM.

Author Contributions: Conceptualization, methodology, investigation, software, validation, writing—original draft preparation, L.A.C.; writing—review and editing, Z.H.; writing—review and editing, H.E.S. All authors have read and agreed to the published version of the manuscript.

Funding: This research received no external funding.

Institutional Review Board Statement: Not applicable.

Informed Consent Statement: Not applicable.

Data Availability Statement: Not applicable.

Conflicts of Interest: The authors declare no conflict of interest.

References

1. Sayler, K.M. *Emerging Military Technologies: Background and Issues for Congress*; Technical Report; Congressional Research Service Washington United States, 2020. Available online: <https://apps.dtic.mil/sti/pdfs/AD1105857.pdf> (accessed on 10 January 2022).
2. Siouris, G.M. *Missile Guidance and Control Systems*; Springer Science & Business Media: New York, NY, USA, 2004.
3. Payne, C.M. *Principles of Naval Weapon Systems*; Naval Institute Press: Annapolis, MD, USA, 2006.
4. GOES-R. GOES-R Series Product Definition and Users' Guide (PUG), 2019, User Readiness Documents. Available online: <https://www.goes-r.gov/resources/docs.html> (accessed on 10 January 2022).
5. Chuvieco, E. *Fundamentals of Satellite Remote Sensing: An Environmental Approach*; CRC Press: Boca Raton, FL, USA, 2016.
6. GOES-R. ABI Full Disk Image. Available online: <https://www.goes-r.gov/spacesegment/abi.html> (accessed on 10 January 2022).
7. Li, J.; Schmit, T.J.; Jin, X.; Martin, G. *GOES-R Advanced Baseline Imager (ABI) Algorithm Theoretical Basis Document for Legacy Atmospheric Moisture Profile, Legacy Atmospheric Temperature Profile, Total Precipitable Water, and Derived Atmospheric Stability Indices*; US Department of Commerce, National Oceanic and Atmospheric Administration, National Weather Service: Washington, DC, USA, 2010.

8. Losos, D. Beginner's Guide to GOES-R Series Data How to Acquire, Analyze, and Visualize GOES-R Series Data. Available online: https://www.goes-r.gov/downloads/resources/documents/Beginners_Guide_to_GOES-R_Series_Data.pdf (accessed on 10 January 2022).
9. Washington, W.M.; Parkinson, C. *Introduction to Three-Dimensional Climate Modeling*; University Science Books: Sausalito, CA, USA, 2005.
10. Chiles, J.P.; Delfiner, P. *Geostatistics: Modeling Spatial Uncertainty*; John Wiley & Sons: Hoboken, NJ, USA, 2009; Volume 497.
11. Devore, J.L. *Probability and Statistics for Engineering and the Sciences*; Cengage Learning: Boston, MA, USA, 2011.
12. Cannon, M.W., Jr.; Carl, J.W. *TERCOM Performance: Analysis and Simulation*; Technical Report; Air Force Aerospace Medical Research Lab Wright-Patterson AFB OH. 1974. Available online: <https://apps.dtic.mil/sti/pdfs/AD0783804.pdf> (accessed on 10 January 2022).
13. Meadows, P.S.; Campbell, J.I. *An Introduction to Marine Science*; Springer Science & Business Media: New York, NY, USA, 2013.